

# Smooth Muscle Specific Rac1 Deficiency Induces Hypertension by Preventing p116<sup>RIP3</sup>-Dependent RhoA Inhibition

Gwennan André, PhD; Juan E. Sandoval, PhD; Kevin Retailleau, PhD; Laurent Loufrani, PhD; Gilles Toumaniantz, PhD; Stefan Offermanns, MD, PhD; Malvyne Rolli-Derkinderen, PhD; Gervaise Loirand, PhD; Vincent Sauzeau, PhD

**Background**—Increasing evidence implicates overactivation of RhoA as a critical component of the pathogenesis of hypertension. Although a substantial body of work has established that Rac1 functions antagonize RhoA in a broad range of physiological processes, the role of Rac1 in the regulation of vascular tone and blood pressure is not fully elucidated.

**Methods and Results**—To define the role of Rac1 in vivo in vascular smooth muscle cells (vSMC), we generated smooth muscle (SM)-specific Rac1 knockout mice (SM-Rac1-KO) and performed radiotelemetric blood pressure recordings, contraction measurements in arterial rings, vSMC cultures and biochemical analyses. SM-Rac1-KO mice develop high systolic blood pressure sensitive to Rho kinase inhibition by fasudil. Arteries from SM-Rac1-KO mice are characterized by a defective NO-dependent vasodilation and an overactivation of RhoA/Rho kinase signaling. We provide evidence that Rac1 deletion-induced hypertension is due to an alteration of cGMP signaling resulting from the loss of Rac1-mediated control of type 5 PDE activity. Consequently, cGMP-dependent phosphorylation and binding of RhoA with its inhibitory partner, the phosphatase-RhoA interacting protein (p116<sup>RIP3</sup>), are decreased.

**Conclusions**—Our data reveal that the depletion of Rac1 in SMC decreases cGMP-dependent p116<sup>RIP3</sup>/RhoA interaction and the subsequent inhibition of RhoA signaling. Thus, we unveil an in vivo role of Rac1 in arterial blood pressure regulation and a new pathway involving p116<sup>RIP3</sup> that contributes to the antagonistic relationship between Rac1 and RhoA in vascular smooth muscle cells and their opposite roles in arterial tone and blood pressure. (*J Am Heart Assoc.*2014;3:e000852 doi: 10.1161/JAHA.114.000852)

**Key Words:** blood pressure • hypertension • nitric oxide • signal transduction • vasoconstriction

The Ras homologous (Rho) family of small GTPases contains 20 members in humans among which RhoA, Rac1, and Cdc42 are the best characterized. One of the major functions of these proteins is the spatial and temporal regulation of the actin cytoskeleton assembly during essential cell processes such as migration, division, and adhesion.<sup>1–3</sup>

From the Inserm UMR\_S1087 CNRS UMR\_C6291 l'institut du thorax Nantes F-44000 France (G.A., J.E.S., G.T., M.R.-D., G.L., V.S.); Université de Nantes Nantes F-44000 France (G.A., J.E.S., G.T., M.R.-D., G.L., V.S.); Inserm UMR\_S1083 CNRS UMR\_C6214 BNMI Angers F-49000 France (K.R., L.L.); Department of Pharmacology Max-Planck-Institute for Heart and Lung Research Bad Nauheim Germany (S.O.); CHU Nantes l'institut du thorax Nantes F-44000 France (G.L., V.S.).

Accompanying Figures S1 through S6 and Table S1 are available at <http://jaha.ahajournals.org/content/3/3/e000852/suppl/DC1>

**Correspondence to:** Vincent Sauzeau, PhD, UMR1087, IRS-UN, 8 quai Moncoussu, 44000 Nantes, France. E-mail: [vincent.sauzeau@inserm.fr](mailto:vincent.sauzeau@inserm.fr)

Received March 31, 2014; accepted April 17, 2014.

© 2014 The Authors. Published on behalf of the American Heart Association, Inc., by Wiley Blackwell. This is an open access article under the terms of the Creative Commons Attribution-NonCommercial License, which permits use, distribution and reproduction in any medium, provided the original work is properly cited and is not used for commercial purposes.

To precisely modulate these cellular functions, the activity of Rho GTPases is finely regulated by mechanisms that include reciprocal negative or positive feedbacks. Typically, numerous studies have revealed a link between RhoA and Rac1 activities. It was initially proposed that activated Rac1 positively regulates RhoA and this finding has been validated in cells from Rac1-deficient mice.<sup>4,5</sup> However, in most situations, Rac1 and RhoA display an antagonistic relationship<sup>6–9</sup> that could result from several different mechanisms affecting their activity, expression and stability, and their downstream signaling pathways.<sup>7</sup>

In the vascular system, Rho GTPases have been increasingly implicated in the regulation of different physiological and mechanoelastic responses. In endothelial cells, RhoA and its main effector Rho kinase negatively regulate NO production by decreasing endothelial nitric oxide synthase (eNOS) expression and activity.<sup>10,11</sup> Rac1 has exactly opposite effects, enhancing eNOS activity and increasing eNOS expression through elevated eNOS mRNA stability and promoting eNOS gene transcription via its effector p21-activated kinase 1 (Pak1).<sup>12,13</sup> This role of Rac1 in endothelial cells was further confirmed in vivo in

endothelial Rac1 haploinsufficient mice (EC-Rac1<sup>+/-</sup>). These mice developed mild hypertension correlated with a decreased expression and activity of eNOS.<sup>12</sup> Endothelial Rac1 was also described to control the production of reactive oxygen species (ROS) and the mobilization of cortical actin network to modulate endothelial permeability.<sup>14–16</sup>

In vascular smooth muscle cells (vSMC), RhoA and Rho kinase are recognized as major regulators of the contraction by inhibiting myosin light chain phosphatase (MLCP), thereby increasing MLC phosphorylation.<sup>17</sup> Accordingly, RhoA/Rho kinase signaling is a key regulator of vascular tone and arterial pressure, and overactivation of RhoA/Rho kinase signaling has been identified as a critical mechanism in the pathogenesis of pulmonary or systemic hypertension.<sup>18</sup> Several vasoconstrictors have also been shown to activate Rac1 in vSMC, however its role in the control of vascular tone is unclear.<sup>19</sup> Rac1/Pak1 signaling has been described to phosphorylate and inhibit MLC kinase, thereby decreasing MLC phosphorylation and smooth muscle cell contraction.<sup>20,21</sup> However, opposite effects have also been reported<sup>22,23</sup> as Pak3, another Rac1 effector, has been shown to enhance smooth muscle contraction through phosphorylation of the thin filament regulatory protein caldesmon.<sup>22,23</sup> In the absence of relevant animal models, the *in vivo* role of vSMC Rac1 in the control of vascular tone and blood pressure remains unknown. In fact, mouse models of ubiquitous deletion of Rac signaling components such as exchange factors of the Vav family display complex cardiovascular phenotypes resulting from multiple defects including sympathetic nervous system and neurohormonal dysfunctions.<sup>24,25</sup>

We therefore generated a new animal model with inducible inactivation of the *Rac1* gene in SMC. We demonstrated that Rac1 deletion in SMC induces high systolic blood pressure in mice through an alteration of cGMP signaling that decreases NO-induced p116<sup>RIP3</sup>/RhoA interaction, leading to a defective NO-mediated RhoA inhibition and vasorelaxation.

## Methods

### Animals Use

All experimental procedures and animal care were performed in accordance with the European Community Standards on the Care and Use of Laboratory Animals and approved by the local ethics committee (Comité d'Éthique en Expérimentation Animale des Pays de Loire). We mated a transgenic mouse line carrying floxed alleles of the gene coding for *Rac1* (*Rac1*<sup>lox/lox</sup>, Jackson Laboratories) to mice expressing a fusion protein of the Cre recombinase with a modified estrogen receptor-binding domain (CreER<sup>T2</sup>) under the control of the

smooth muscle myosin heavy chain (SMMHC) promoter (SMMHC-CreER<sup>T2</sup> mice)<sup>26,27</sup> to produce *SMMHC-CreER*<sup>T2</sup>; *Rac1*<sup>lox/lox</sup> mice (SM-Rac1<sup>lox/lox</sup> mice). The recombinase Cre was activated in 2-month-old mice by intraperitoneal injection of tamoxifen (1 mg/day dissolved in sun-flower oil, T5648, Sigma) for 5 consecutive days during 2 weeks. Male mice were analyzed 1 month after tamoxifen treatment. *Rac1*<sup>lox/lox</sup> mice treated with tamoxifen and SM-Rac1<sup>lox/lox</sup> mice without tamoxifen treatment were used as control animals. In this study, 85 SM-Rac1<sup>lox/lox</sup> and 95 *Rac1*<sup>lox/lox</sup> mice were used for functional analyses.

### Immunoblot Analysis

vSMC or cleaned aortas were incubated on ice with lysis buffer supplemented with proteases and phosphatases inhibitors cocktails (Sigma) and sodium orthovanadate. Lysates were subjected to SDS-PAGE, transferred to nitrocellulose membranes and incubated with specific antibodies. Immune complexes were detected with appropriate secondary antibodies and enhanced chemiluminescence reagent (ECL plus; GE Healthcare). Protein band intensities were quantified using ImageJ Software (NIH software).

### Histological Analysis

Hearts, kidneys, and aortas were fixed in 4% paraformaldehyde in PBS and embedded into paraffin. We stained 6 μm sections with hematoxylin and eosin (Sigma). Aorta media wall thickness and cellular density were quantified in a blind manner using Metamorph-Metaview software (Universal Imaging).

### Arterial Pressure Measurements

Blood pressure was measured in conscious and unrestrained mice using a radiotelemetry system as described previously<sup>28</sup> (PA-C10 and Dataquest software; Data Sciences International). L-NAME treatment (N5751; Sigma) was administered in the drinking water (300 mg/kg of body weight/day) and renewed every 3 days. The recording room was maintained with a 12-hour-light/12-hour-dark cycle. Blood pressure was also measured in restrained mice with a noninvasive tail-cuff device (BP 2000; Visitech Systems). Fasudil treatment (F4660; LC laboratories) was administered by intraperitoneal injection (5 or 30 mg/kg of body weight) 20 minutes before measurements.

### Echocardiography

Two-dimensional (2-D) echocardiography was performed on mice using a Vivid 7 Dimension ultrasonography (GE

Healthcare) with a 14-MHz transducer. Left ventricular free wall thickness, anterior wall, and posterior wall thickness were measured during diastole and systole from long- and short-axis images obtained by M-mode echocardiography. Transmitral flow measurements of ventricular filling velocity were obtained using pulsed Doppler, with an apical four-chamber orientation. Thus, early diastolic (E), late diastolic (A), and the ratio, E/A were obtained to assess diastolic dysfunction. To avoid bias in the analysis, blind experiments were done and scored by members of our research team.

## Renal Function

Physiocages were used to evaluate urine production during 48h after a 3-day acclimatizing period. Urines were collected and analyzed at the ONIRIS laboratory facility (Nantes, France) to determine creatinine clearance and  $\text{Na}^+$  concentration.

## Arterial Reactivity

To analyze the pressure and the flow-dependent tone, segments of first-order mesenteric arteries were removed and cannulated at both ends in a video-monitored perfusion system (Living System Instrumentation) as previously described.<sup>29</sup> Briefly, arteries were bathed and perfused with a physiological salt solution. To assess myogenic tone, diameter changes were measured when intraluminal pressure was set from 10 to 125 mm Hg without intraluminal flow (active diameters). At the end of each experiment, arterial segments were superfused with a  $\text{Ca}^{2+}$ -free physiological salt solution containing EGTA (2 mmol/L), sodium nitroprusside (10  $\mu\text{mol/L}$ ) and papaverin (10  $\mu\text{mol/L}$ ), and pressure steps (10 to 125 mm Hg) were repeated (passive diameter). Myogenic tone was expressed as active tone (passive diameter – active diameter) in percentage of passive diameter. For flow-dependent tone, arteries were submitted to a 75 mm Hg pressure and precontracted with phenylephrine (Phe; 0.3 to 1  $\mu\text{mol/L}$ ) to maintain a stable tone ( $\approx 50\%$  of the maximum response). Intraluminal flow was increased by step (0 to 100  $\mu\text{L/min}$ ) and diameter measured. Flow-mediated relaxation was expressed as the percentage of dilation of the active tone (precontraction).

To analyze aortic and mesenteric arterial vasoreactivity, 2-mm-long rings were cut, cleaned, and mounted on a multichannel isometric myograph (Danish Myo Technology) containing a Krebs-Henseleit solution (in mmol/L: 118.4 NaCl, 4.7 KCl, 2  $\text{CaCl}_2$ , 1.2  $\text{MgSO}_4$ , 1.2  $\text{KH}_2\text{PO}_4$ , 25  $\text{NaHCO}_3$ , and 11 glucose). We constructed cumulative concentration-response curves in response to KCl, Phe, and the thromboxane A2 receptor agonist (U46619). Relaxation-response curve in

response to carbachol (CCh), S-Nitroso-N-Acetyl-DL-Penicillamine (SNAP), and isoprenaline (IsoP) were constructed after Phe precontraction. When indicated, rings were pretreated with L-NAME (100  $\mu\text{mol/L}$ ) 1 hour before contraction measurements. Chamber wire myograph was connected to a digital data recorder (MacLab/4e; AD Instruments) and recordings were analyzed using LabChart v7 software (AD Instruments).

## NO Signaling Pathway Analysis

Plasmatic nitrites concentration was determined using Griess Reagent Kit (Molecular probes; Invitrogen). cGMP and cAMP concentrations were evaluated in aorta and transfected vSMC according to the supplier's specifications (Cyclic GMP and AMP EIA Kit; Cayman Chemical).

## Analysis of Rac1 and RhoA Activity

Pull-down assay using GST-PBD or GST-RBD fusion proteins were performed on fresh vSMC or aorta lysates to evaluate Rac1 and RhoA activities, respectively.<sup>30</sup>

## Cell Culture, Transfection and Actin Staining

Primary aortic smooth muscle cells were isolated and cultured as described previously.<sup>31</sup> cDNA coding for wild-type Rac1 (Rac<sup>WT</sup>), wild-type RhoA (GFP-RhoA<sup>WT</sup>), constitutive inactive form of Rac1 (Rac<sup>N17</sup>), constitutive active Rac1 (Rac<sup>V12</sup>), phospho-mimetic RhoA (GFP-RhoA<sup>S188E</sup>), and phospho-resistant RhoA (GFP-RhoA<sup>S188A</sup>) were transfected in vSMC with jetPEI (Polyplus transfection) according to the manufacturer's instructions. To selectively knockdown the expression of endogenous p116<sup>RIP3</sup>, two siRNA oligonucleotides were designed (Eurogentec): siRNA1 5'-GGUCCAGGUAAUUGAGAA+dTdT-3' and siRNA2 5'-GAG-CACAUGGAAACCAACA+dTdT-3'. RNA duplexes or a siRNA negative control oligonucleotide (SR-CL000-005; Eurogentec) were transfected by Lipofectamine RNAiMAX (Invitrogen) according to the supplier's specifications. When indicated, cells were treated 1 hour with SNP (10  $\mu\text{mol/L}$ ), IsoP (10  $\mu\text{mol/L}$ ) or 8-Br-cGMP (100  $\mu\text{mol/L}$ ). After treatments, vSMC were fixed with 4% paraformaldehyde in PBS, permeabilized in PBS 0.5% Triton X-100, and incubated with 130  $\mu\text{g/mL}$  of FITC-conjugated phalloidin (Sigma) or 5 mg/mL of Texas red-DNaseI (Molecular Probes; Invitrogen) to visualize F-actin and monomeric G-actin, respectively. After staining, images were captured by a fluorescence microscope (Nikon) and quantified using Metamorph-Metaview software (Universal Imaging). The ratio of fluorescence of FITC-phalloidin and Texas red-DNaseI (F-actin/G-actin ratio) was used to quantify the actin cytoskeleton organization.

## Co-Immunoprecipitation

Immunoprecipitation of RhoA in aorta to reveal p116<sup>RIP3</sup> was carried out with a polyclonal RhoA antibody (1/500) using A-protein magnetic beads ( $\mu$ MACS 130-071-001; Milteny) according to the supplier's specifications. Anti-GFP-beads ( $\mu$ MACS 130-091-125; Milteny) were used for GFP immunoprecipitation. The coimmunoprecipitations for the others were performed with anti-Pak1 (1/500) or anti-PKG (1/1000) antibodies and G-Sepharose beads (fast-flow; GE Healthcare) overnight at 4°C followed by washes with the lysis buffer.

## Chemicals and Antibodies

Antibodies against Rac1 (610651) and eNOS/NOS (610297) were from BD Biosciences. Anti-MYPT1 (2634), P-Pak (2605), Pak1 (2602), PDE5 (2395), PKG (3248), and RhoA (2117) antibodies were from Cell Signaling Technology. Anti-P-MYPT (sc17556), p116<sup>RIP3</sup> (sc135494) and P<sup>Ser188</sup>-RhoA (sc32954) antibodies were from Santa Cruz Biotechnology. Anti-soluble guanylyl cyclase sGC $\alpha$ 1 (G4280) and sGC $\beta$ 1 (G4405) antibodies were from Sigma. Anti-eGFP antibody was from Clontech (632569). All agonists used for the analysis of blood vessels reactivity and vSMC treatment were from Sigma when not specified.

## Statistics

Results are expressed as the mean $\pm$ SEM of sample size *n*. Statistical analysis were performed with either the 2-tailed Student's *t* test or the 1-way ANOVA test. For small sample sizes, a nonparametric test (Mann-Whitney) was applied. A value of *P*<0.05 or less was considered to be statistically significant.

## Results

### Generation of Mice With Smooth Muscle-Specific Rac1 Deficiency

Mice specifically lacking Rac1 in SMC (SM-Rac1-KO mice) were obtained by treating SM-Rac1<sup>lox/lox</sup> mice with tamoxifen. Wild-type and floxed Rac1 alleles were identified by PCR (WT, 115 bp; floxed, 242 bp) and Cre-mediated recombination generated a 140 bp band allowing the identification of SM-Rac1-KO mice (Figure S1A). In situ hybridization and RT-PCR confirmed the inhibition of *Rac1* mRNA expression in vSMC from SM-Rac1-KO mice (Figure S1B and S1C). Likewise, Rac1 protein was poorly detected by immunoblot and immunohistochemistry in aortic vSMC from SM-Rac1-KO mice (Figure S1D and S1E).

### Rac1-Deficient Mice Develop High Systolic Blood Pressure

The impact of SM Rac1 deletion on blood pressure and heart rate was evaluated by radiotelemetry. Before treatment with tamoxifen, baseline heart rate, systolic, diastolic and mean arterial blood pressures were similar in control and SM-Rac1<sup>lox/lox</sup> mice (Figures 1A, 1B, S2A, and S2B). Tamoxifen treatment was rapidly followed by an increase in systolic blood pressure in SM-Rac1-KO mice (Figure 1A). One month after induction of Rac1 deletion in SMC, systolic blood pressure was significantly higher in SM-Rac1-KO mice compared to tamoxifen-treated Rac1<sup>lox/lox</sup> mice (Figure 1B; Table) and SM-Rac1<sup>lox/lox</sup> mice without treatment (data not shown), during both 12-hour-dark and 12-hour-light periods. This difference in systolic blood pressure was maintained over time (Figure S3B) and was not associated with change in diastolic blood pressure and heart rate (Figures S2A and S2B and Table). SM-Rac1-KO mice developed thickening of the aortic wall typical of the hypertensive remodeling observed in mice models,<sup>24,25</sup> and patients with high blood pressure<sup>24,25,32</sup> (Figure S3A; and Table). At the cardiac level, echo Doppler measurements revealed that left ventricle thickness was slightly enlarged indicating cardiac hypertrophy initiation in response to the elevated systolic blood pressure (Table). However, the heart weight to body weight ratio was similar in SM-Rac1-KO and Control mice (Table). Measurements of blood pressure in 14-month-old SM-Rac1-KO mice showed persistent high blood pressure, without any sign of myocardial fibrosis (Figure S3B and S3C).

Analysis of the renal function that plays a major role in the regulation of blood pressure, showed that glomerular filtration rate (creatinine clearance) and excretion rate of Na<sup>+</sup> were not altered in SM-Rac1-KO mice (Table). Moreover, histological analysis did not reveal any structural remodeling such as renal fibrosis or glomerulosclerosis in 14-month-old SM-Rac1-KO compared with control mice (Figure S3C). These data thus suggest that the rise in systolic pressure in SM-Rac1-KO mice is not related to renal dysfunction.

### Rac1 Deficiency in SMC Leads to Impaired NO-Dependent Vasodilation

To shed light on the origin of high systolic blood pressure, we explored the functional properties of SM-Rac1-KO arteries. Arterial diameters were similar in both group of mice, but a slight increase of elastance was observed in mesenteric arteries from SM-Rac1-KO mice compared to control mice (Table). Pressure-induced tone (myogenic tone) was not affected by SMC Rac1 deletion (Figure 2A). The contractile response to KCl was similar in the aorta, mesenteric, and

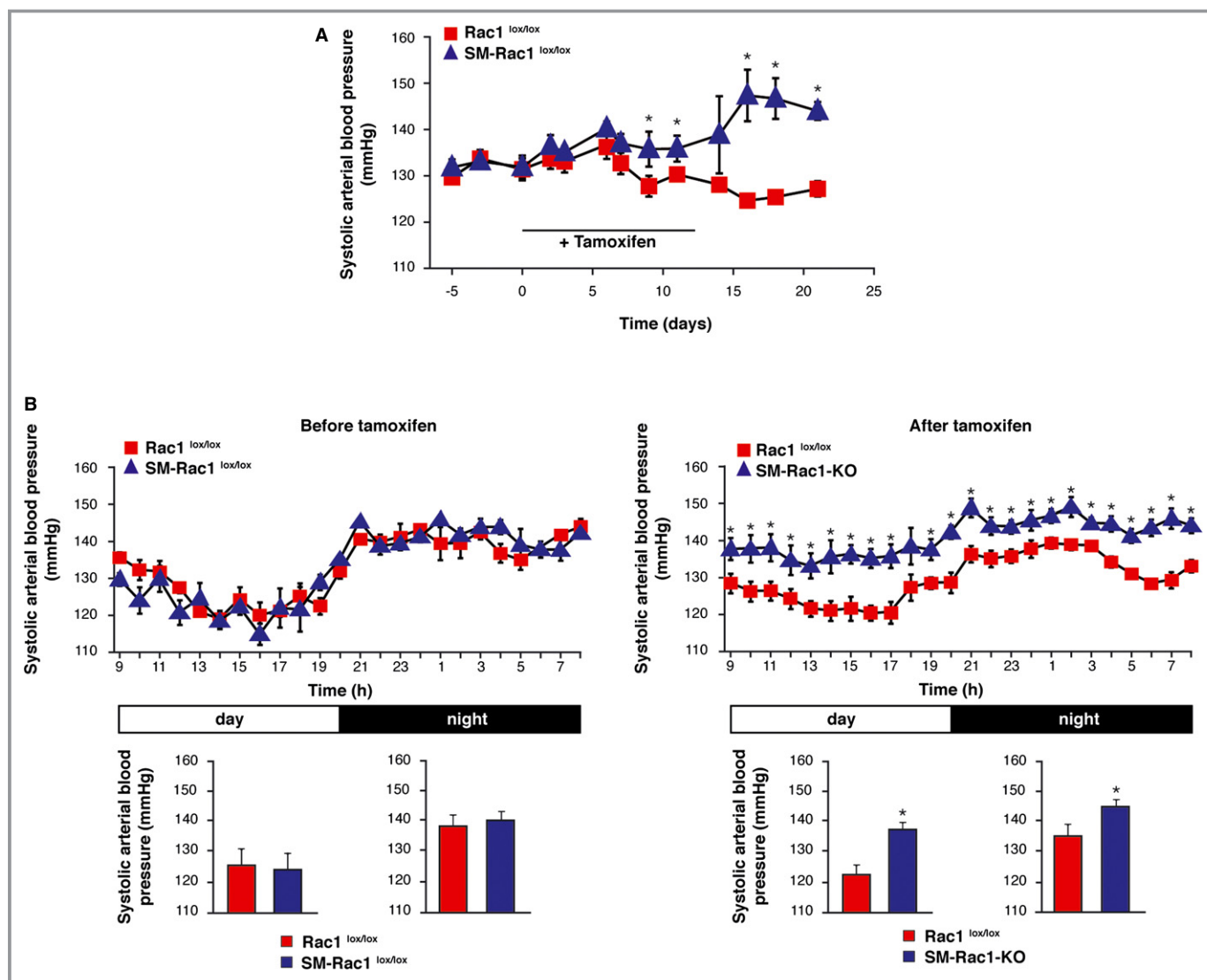


**Figure 1.** Rac1 deficiency in SMC induces an increase of systolic arterial blood pressure. A, Telemetric records of systolic blood pressure in Rac1<sup>lox/lox</sup> (n=8) and SM-Rac1<sup>lox/lox</sup> (n=9) mice. Tamoxifen treatment period to induce Rac1 deletion is indicated. B, Profiles over 24 hours of systolic blood pressure. Measurements were performed under a 12:12-hour light/dark schedule. Left panels represent analysis before induction of Rac1 deletion and right panels after tamoxifen treatment (n=8 to 9). \*P<0.05. SM-Rac1 indicates smooth muscle Rac1 knockout.

renal arteries from SM-Rac1-KO mice compared with control mice (Figures S4, S5A, and S6A). The responses to the thromboxane A2 analog (U46619) and phenylephrine (Phe) were slightly increased in mesenteric arteries from SM-Rac1-KO mice (Figures S4 and S5A). In contrast, flow-induced relaxation was significantly reduced in mesenteric resistance arteries from SM-Rac1-KO mice as compared to Rac1<sup>lox/lox</sup> mice (Figure 2B). Flow-mediated dilation mainly depends on the capacity of vSMC to respond to flow-induced endothelium-derived vasodilator agents such as nitric oxide (NO) and cyclooxygenase-mediated prostacyclins. The altered relaxation observed in arteries from SM-Rac1-KO mice suggests that Rac1 might be involved in response to these vasodilator factors.

To test this hypothesis, the endothelial-mediated relaxation was assessed by testing the vasodilatory effect of carbachol (CCh) in arterial rings pre-contracted with Phe. This relaxation response was impaired in both aorta and mesenteric arteries from SM-Rac1-KO mice (Figures 2C and 2D, S5B). CCh promotes vasodilation by inducing NO release and endothelium-derived hyperpolarization factors (EDHF) production. To determine the relaxing pathways affected by Rac1 deletion, we first inhibited NO signaling by the NO synthase (NOS) inhibitor, L-NAME. L-NAME reduced the relaxing effect of CCh in mesenteric arteries from control but not in those from SM-Rac1-KO mice. In the presence of L-NAME, the relaxing effect of CCh was the same in WT and SM-Rac1-KO mice arteries (Figure 2D). Similarly, in vivo treatment with L-NAME

**Table.** Cardiovascular Parameters in Rac1<sup>lox/lox</sup> and SM-Rac1-KO Mice

	Rac1 <sup>lox/lox</sup>	SM-Rac1-KO	P Value	n
Body weight, g	27.2±0.6	27.1±0.8	0.46	22
Restrained systolic ABP, mm Hg	102±3	120±4	0.01*	10
Telemetric systolic ABP (mm Hg) (24 hours)	127±2	142±3	0.02*	9
Telemetric diastolic ABP (mm Hg) (24 hours)	95±1	97±2	0.19	9
Relative aorta media wall thickness	1.0±0.07	1.33±0.07	0.02*	4
Relative aortic cellular density	1.0±0.06	1.23±0.03	0.01*	4
Aortic diameter, μm	417±16	407±19	0.29	8
Mesenteric artery diameter, μm	188±12	192±8	0.35	8
Aortic elastance (% control)	100±8	104±5	0.28	8
Mesenteric artery elastance (% control)	100±4	120±6	0.01*	8
Heart (mg)/body weight (g)	4.9±0.3	4.8±0.1	0.24	7
LV systolic thickness, mm	1.78±0.06	2.08±0.17	0.12	8
LV diastolic thickness, mm	1.26±0.07	1.69±0.15	0.02*	8
Heart rate, bpm	532±21	564±9	0.20	8
E/A ratio	1.47±0.07	1.18±0.07	0.01*	8
Kidney weight, mg	180±1	183±4	0.30	4
Creatinine clearance, mL min <sup>-1</sup> kg <sup>-1</sup>	4.29±0.53	3.82±0.45	0.34	6
FE <sub>Na</sub> , %	0.44±0.03	0.45±0.05	0.38	6

Arterial characteristics were monitored either by tail-cuff, telemetry, histological or myograph measurements. Cardiac parameters were obtained by echocardiography. Renal function was assessed by sodium and creatinine related dosages. All parameters were measured 1 month after Rac1 deletion. ABP indicates arterial blood pressure; E/A, early diastolic (E), late diastolic (A), LV, left ventricle; FE<sub>Na</sub>, fractional sodium excretion; n, sample size per group; SM-Rac1, smooth muscle Rac1 knockout.

\*P<0.05 Rac1<sup>lox/lox</sup> vs SM-Rac1-KO mice.

increased systolic blood pressure in control mice but had no significant effect in SM-Rac1-KO mice (Figure 2E). Consequently, after L-NAME treatment, systolic arterial blood pressure was similar in both groups of mice (Figure 2E), supporting that NO signaling deficiency contributes to the vascular defects and the increased systolic pressure observed in SM-Rac1-KO mice. These ex vivo and in vivo data thus suggest that EDHF signaling pathway was not altered in SM-Rac1-KO mice and that the reduced CCh-induced relaxation in arteries from SM-Rac1-KO-mice likely resulted from a defective vSMC response to endothelial NO.

This hypothesis was confirmed by the use of the NO donor SNAP. The relaxing effect of increasing concentrations of SNAP was strongly decreased in arterial rings from SM-Rac1-KO mice compared to that obtained in control rings (Figures 2D, S5B, and S6B). In contrast, the relaxation induced by the β-adrenergic receptor agonist isoprenaline (IsoP), that is mediated by increased production of cAMP in vSMC, was similar in arteries from control and SM-Rac1-KO mice (Figures 2D and S5B). All these results indicate that Rac1 deletion causes a specific primary defect in signaling pathways responsible for relaxing response to endothelial NO in vSMC. This conclusion is further supported by the observation that the NO production, estimated by measuring

the plasma nitrite concentration, was similar in control and SM-Rac1-KO mice at 5 and 15 days after induction of Rac1 deletion in SMC, while systolic blood pressure was already increased (Figure 2F).

### Rac1 Deletion Leads to Defective Production of cGMP in vSMC

We next wanted to understand the mechanism linking Rac1 deletion in SMC to a defective response to NO. Western-blot analysis revealed that the expression of the main molecular components of the NO pathway, endothelial NOS (eNOS), soluble guanylyl cyclases (sGC) α1 and β1, type 5 phosphodiesterase (PDE5), and cGMP-dependent protein kinase (PKG), was not affected by Rac1 deletion in vSMC (Figure 3A). However, 15 days after the end of tamoxifen treatment, we observed a 50% reduction of the cyclic Guanosine Monophosphate (cGMP) content in SM-Rac1-KO mouse arteries compared to those of control animals (Figure 3B). The concentration of cAMP, another second messenger leading to vasodilation, was similar in both groups of mice (Figure 3B). These results suggest that the defective response to NO in SM-Rac1-KO mice arteries resulted from a reduction of NO-induced rise in cGMP in vSMC. This hypothesis was confirmed

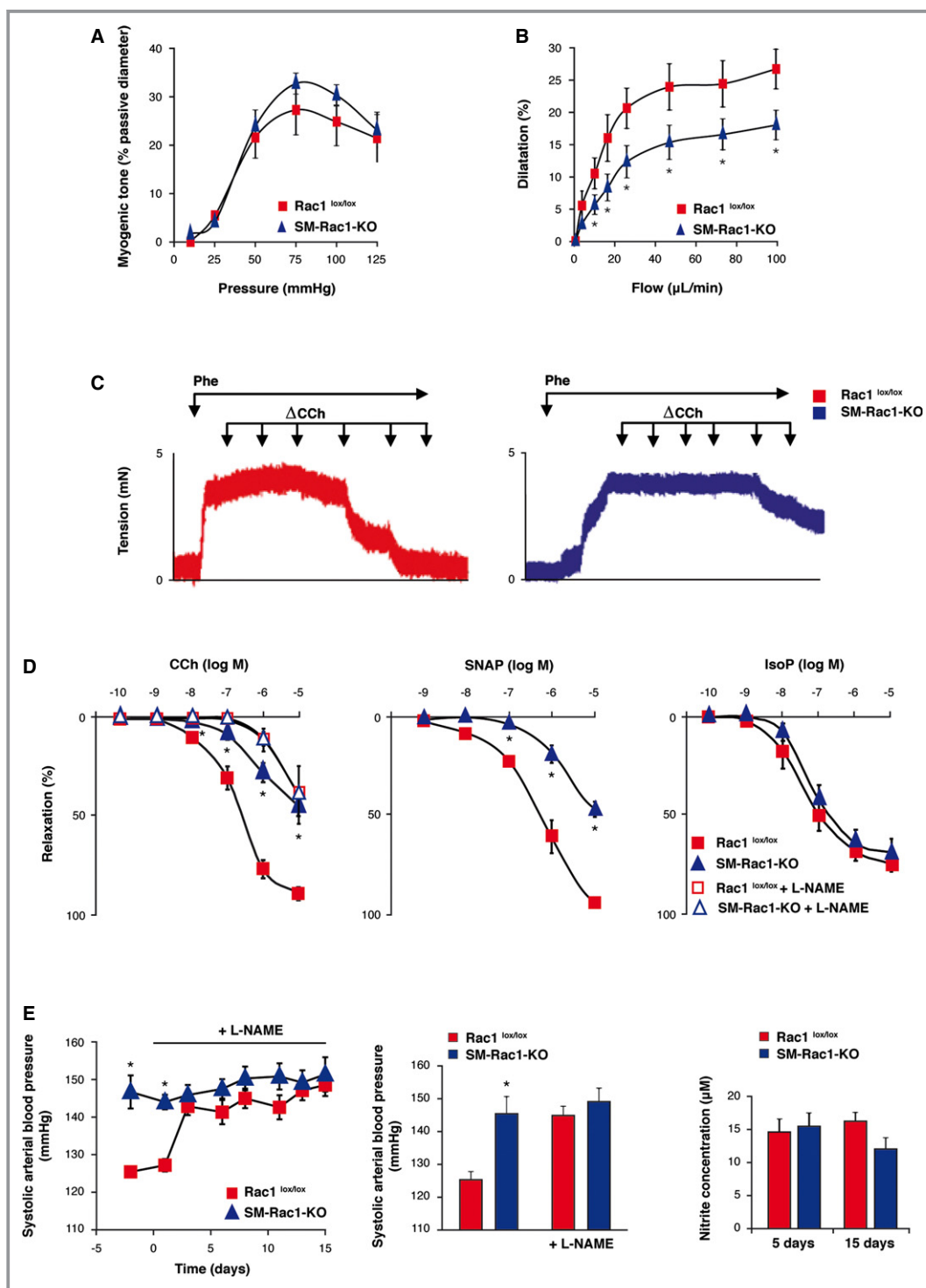


**Figure 2.** NO-dependent relaxation is impaired in SM-Rac1-KO mice. A, Pressure-induced myogenic tone and (B) flow-induced vasodilation in mesenteric arteries from  $Rac1^{lox/lox}$  and SM-Rac1-KO mice (n=8). C, Representative real-time recordings of the response of Phe-constricted mesenteric arteries to cumulative administration (arrows) of CCh ( $10^{-10}$  to  $10^{-5}$  mol/L). D, Percentage of vessel relaxation induced by the indicated doses of CCh, SNAP and IsoP on Phe-constricted mesenteric arteries from  $Rac1^{lox/lox}$  and SM-Rac1-KO mice pretreated or not with L-NAME (1 hour, 100 μmol/L; n=5 to 12). E, Systolic blood pressure in  $Rac1^{lox/lox}$  (n=8) and SM-Rac1-KO (n=9) mice chronically treated with L-NAME (300 mg/kg of body weight/day in drinking water). F, Plasma nitrite measurements 5 and 15 days after tamoxifen treatment (n=5 to 10). Log M, logarithm of the molar concentration used for each agent. \* $P < 0.05$  compared with controls. CCh indicates carbachol; IsoP, isoprenaline; NO, nitric oxide; SM-Rac1, smooth muscle Rac1 knockout; SNAP, S-Nitroso-N-Acetyl-DL-Penicillamine.

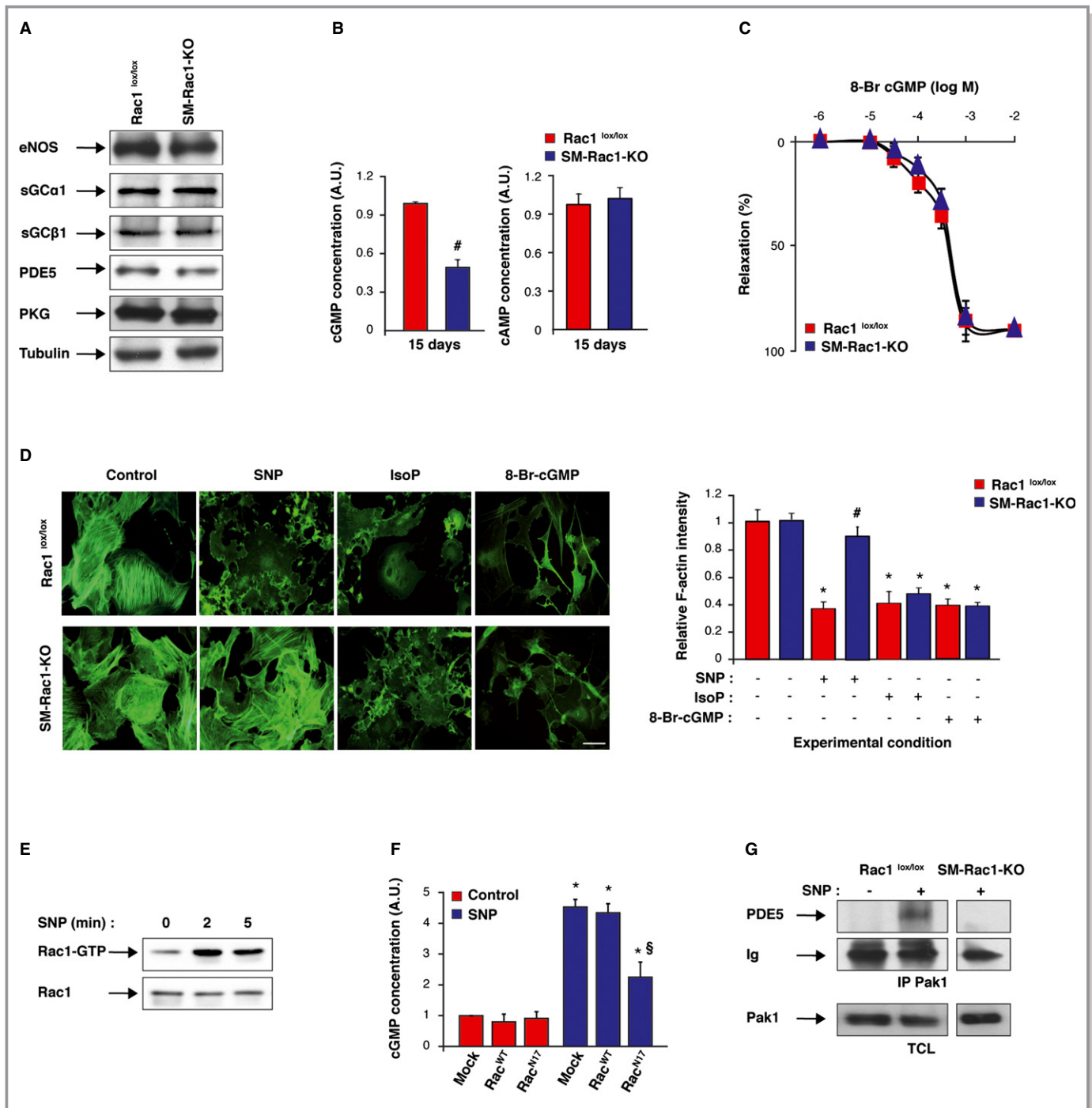


**Figure 3.** Rac1 is essential for NO-dependent cGMP production in vSMC. **A**, Immunoblot analysis of eNOS, sGC $\alpha$ 1, sGC $\beta$ 1, PDE5, and PKG protein expression in Rac1<sup>lox/lox</sup> and SM-Rac1-KO aortas (n=3). **B**, Level of cGMP and cAMP contents in aorta from the indicated mouse strains 15 days after tamoxifen treatment (n=6 to 7). **C**, Percentage of vessel relaxation induced by the indicated doses of the cGMP analogue 8-Br cGMP on Phe-constricted mesenteric arteries from Rac1<sup>lox/lox</sup> and SM-Rac1-KO mice (n=5). Log M, logarithm of the molar concentration used. **D**, Left panel, representative images of the F-actin cytoskeleton in Rac1<sup>lox/lox</sup> and SM-Rac1-KO vSMC after treatment with the indicated drugs (scale bar 20  $\mu$ m). Right panel, corresponding quantification of F-actin/G-actin ratio (n=3). **E**, Pull-down analysis of Rac1 activation by SNP in vSMC. **F**, Production of cGMP after SNP treatment in vSMC transfected with the indicated Rac1 mutants (n=3). **G**, Detection by western blot of PDE5 in anti-Pak1 immunoprecipitates obtained from Rac1<sup>lox/lox</sup> and SM-Rac1-KO aortas treated or not with SNP (n=6). #*P*<0.01 compared with Rac1<sup>lox/lox</sup> control; \**P*<0.05 compared with the same condition without drug; §*P*<0.05 compared with Rac<sup>WT</sup> with SNP. cGMP indicates cyclic Guanosine MonoPhosphate; eNOS, endothelial nitric oxide synthase; IP, immunoprecipitation; Ig, Immunoglobulin; IsoP, isoprenaline; NO, nitric oxide; PAK1, p21-activated kinase 1; PDE5, type 5 phosphodiesterase; PKG, protein kinase G; sGC, soluble guanylyl cyclases; SM-Rac1, smooth muscle Rac1 knockout; TCL, total cell lysate; vSMC, vascular smooth muscle cells.

by the use of the cell-permeable cGMP analog (8-Br-cGMP) that induced a similar vasodilation in mesenteric arteries rings from control and SM-Rac1-KO mice (Figure 3C).

To directly address the role of Rac1 downstream of NO in vSMC, we assessed the ability of NO to promote cGMP-dependent disassembly of F-actin in vSMC.<sup>33</sup> In control condition, F-actin level was similar in vSMC from Rac1<sup>lox/lox</sup> and SM-Rac1-KO mice (Figure 3D). As expected, the NO donor sodium nitroprussiate (SNP) induced stress fiber disassembly in vSMC from Rac1<sup>lox/lox</sup> mice, but had no effect on vSMC from SM-Rac1-KO mice (Figure 3D). In contrast, the cAMP-elevating agent IsoP or 8-Br-cGMP induced a same stress fiber disassembly in both control and Rac1-KO vSMC (Figure 3D), thus confirming a role of Rac1 in NO signaling upstream of cGMP production in vSMC. In fact, we observed that SNP induced Rac1 activation in vSMC (Figure 3E) and that expression of a dominant negative Rac1 mutant (Rac1<sup>N17</sup>) significantly inhibited SNP-induced increase in cGMP in vSMC (Figure 3F), indicating that Rac1 activation is necessary for NO-induced rise in cGMP. The effector of Cdc42 and Rac1 proteins Pak1 has been shown to interact in vitro with PDE5 thereby limiting its cGMP-hydrolyzing activity.<sup>34</sup> To assess the potential role of PDE5 in the reduced cGMP response to NO donors in Rac1-deficient vSMC, we analyzed the Pak1/PDE5 interaction in control and SM-Rac1-KO mice arteries. Activation of NO signaling by SNP induced the formation of the Pak1/PDE5 complex in aortas from control mice but not in those from SM-Rac1-KO mice (Figure 3G). These results suggest that Rac1 deletion in vSMC prevents Pak1-mediated PDE5 inhibition, thus leading to a reduced cGMP level and vasodilation in response to NO.

### Rac1 Deletion Induced RhoA/Rho Kinase Signaling Overactivation

Inhibition of RhoA/Rho kinase signaling is one of the main mechanisms by which NO mediates vasodilation through cGMP/PKG-dependent RhoA phosphorylation on serine 188 (P<sup>Ser188</sup>-RhoA).<sup>33</sup> To determine the role of RhoA/Rho kinase activation in the hypertensive SM-Rac1-KO phenotype, mice were treated with the Rho kinase inhibitor fasudil (at 5 or 30 mg/kg of body weight). Twenty minutes after fasudil injection, systolic arterial pressure was decreased to the same level in both groups of mice, suggesting that the rise in blood pressure in SM-Rac1-KO mice was mediated by an increase in RhoA/Rho kinase activity (Figure 4A). Immunoblot analysis in aorta revealed that the depletion of Rac1 in SM-Rac1-KO aorta was associated with a loss of phosphorylated (active) Pak1 (P-Pak1) but had no effect on RhoA or MYPT expression (Figure 4B). However, the amount of P<sup>Ser188</sup>-RhoA was decreased and the level of P-MYPT was increased in SM-Rac1-KO mice aorta compared with control (Figure 4B). These

results indicate an upregulation of RhoA/Rho kinase activity in arteries of SM-Rac1-KO mice suggesting that NO-mediated Rac1 activation tonically antagonizes RhoA/Rho kinase activity.

### Rac1 Deletion Disrupts p116<sup>RIP3</sup>-RhoA Association

In order to identify Rac1 interacting partners or effectors other than Pak1 involved in NO-induced RhoA/Rho kinase inactivation, we performed Rac1-GST pull-down assay in control and SNP-treated vSMC. After two-dimensional gel electrophoresis and Coomassie blue staining, spots modified by SNP treatment were identified by mass spectrometry. We thus caught the Myosin Phosphatase Rho-Interacting Protein (p116<sup>RIP3</sup>), whose interaction with Rac1 was decreased by SNP (Table S1). Western blot analysis of p116<sup>RIP3</sup> in Rac1 immunoprecipitate confirmed this result (Figure 5A). Interaction of p116<sup>RIP3</sup> with Rac1<sup>WT</sup> was similar to that observed with the dominant active Rac1<sup>V12</sup> and the dominant negative Rac1<sup>N17</sup> mutants (Figure 5B), indicating that p116<sup>RIP3</sup>-Rac1 association did not depend on SNP-induced Rac1 activation.

Interestingly, p116<sup>RIP3</sup> was identified as a RhoA inhibitor that directly interacts with RhoA in a nucleotide-independent manner and also with PKG in human vSMC.<sup>35</sup> As a mirror image of its dissociation from Rac1, SNP promoted p116<sup>RIP3</sup>-RhoA interaction (Figure 5A). In contrast, although the p116<sup>RIP3</sup>-PKG complex was not modified by SNP stimulation (Figure 5C), the kinetic of SNP-induced RhoA-p116<sup>RIP3</sup> complex formation paralleled SNP-induced RhoA phosphorylation (Figure 5D). Expression of wild-type (RhoA<sup>WT</sup>), phosphomimetic (RhoA<sup>S188E</sup>) or phospho-resistant (RhoA<sup>S188A</sup>) RhoA mutant in vSMC showed that under resting condition, p116<sup>RIP3</sup> was more strongly bound to RhoA<sup>S188E</sup> than to RhoA<sup>WT</sup> (Figure 5E). Furthermore, SNP increased the interaction of p116<sup>RIP3</sup> with RhoA<sup>WT</sup> but not with the phospho-resistant RhoA<sup>S188A</sup> mutant (Figure 5E). These results indicate that phosphorylation of RhoA on Ser188 favors its interaction with its inhibitor p116<sup>RIP3</sup>.

We then wanted to assess the role of p116<sup>RIP3</sup> in NO-induced RhoA inactivation by siRNA-mediated p116<sup>RIP3</sup> silencing in vSMC (Figure 6A). The down-regulation of p116<sup>RIP3</sup> expression did not affect NO-induced RhoA phosphorylation but strongly reduced NO-induced actin stress fiber disruption (Figures 6B and 6C) suggesting that the interaction of phosphorylated RhoA with p116<sup>RIP3</sup> is required for the inhibitory action of NO on RhoA/Rho kinase signaling. The next question was therefore to know whether p116<sup>RIP3</sup> was involved in the alteration of NO signaling and the up-regulation of RhoA/Rho kinase pathway induced by Rac1 deletion in SM-Rac1-KO mice arteries. Co-immunoprecipitation experiments demonstrated that p116<sup>RIP3</sup> was associated

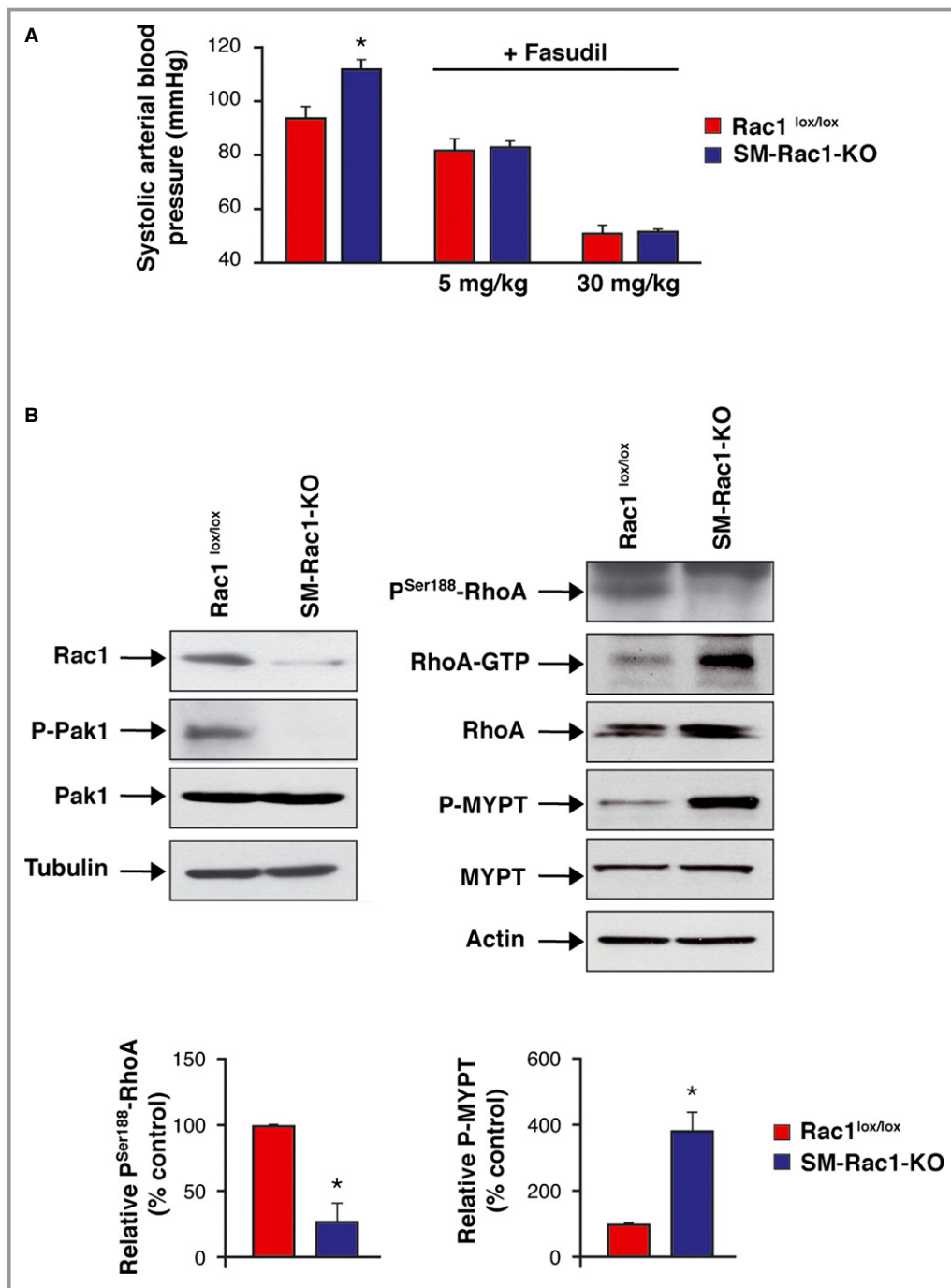


**Figure 4.** Over activation of RhoA/Rho kinase signaling in Rac1 deficient arteries. A, Tail-cuff measurements of systolic arterial blood pressure 20 minutes after i.p. vehicle or fasudil treatment in vivo (5 or 30 mg/kg of body weight). B, Top panel, immunoblot analysis of Rac1/Pak1 and RhoA/Rho kinase pathways in aortas from Rac1<sup>lox/lox</sup> and SM-Rac1-KO mice (n=3 to 4). Bottom panel, corresponding quantification of Ser188 RhoA and MYPT phosphorylation. \* $P < 0.05$ . PAK1 indicates p21-activated kinase 1; Rho, Ras homologous; SM-Rac1, smooth muscle Rac1 knockout.

with RhoA in aorta of control mice but not in those from SM-Rac1-KO mice (Figure 6D). In agreement with the positive effect of NO donors observed in vitro, the inhibition of NO production by L-NAME decreased p116<sup>RIP3</sup>-RhoA interaction in control mice, but had no effect in SM-Rac1-KO mice

(Figure 6D). Thus, these results suggest that Rac1 is required for NO-induced RhoA-p116<sup>RIP3</sup> interaction and are consistent with the involvement of the disruption of the RhoA-p116<sup>RIP3</sup> complex in the activation of RhoA/Rho kinase signaling in SM-Rac1-KO mice arteries.

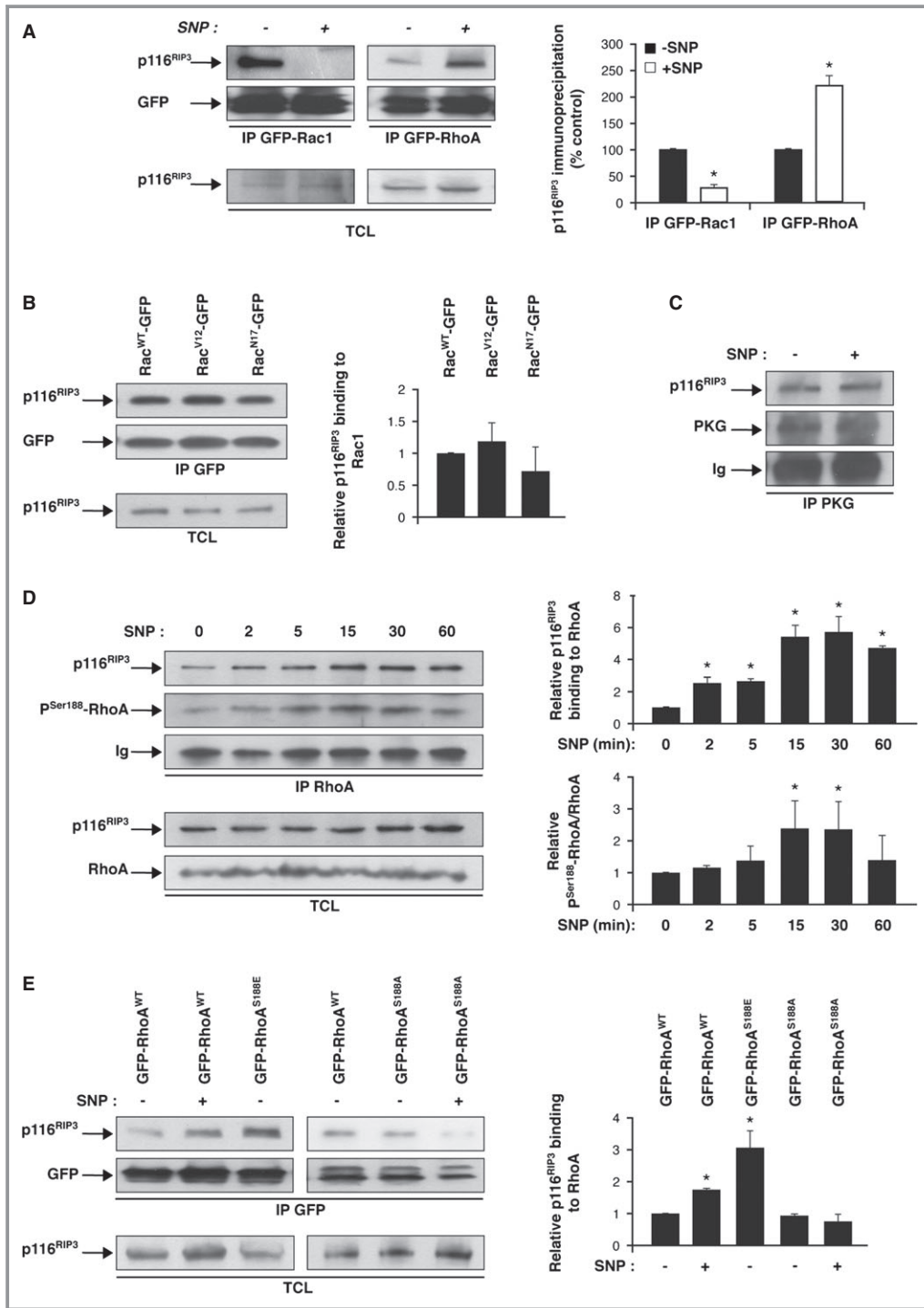


**Figure 5.** NO signaling modulates association between RhoA and its inhibitor p116<sup>RIP3</sup>. A, Left panel, p116<sup>RIP3</sup>-Rac1 and p116<sup>RIP3</sup>-RhoA complexes were analyzed by Western blotting of each GTPase immunoprecipitates (IP GFP) from GFP-Rac1WT and GFP-RhoAWT transfected vSMC treated or not with SNP (n=3 to 4). Right panel, quantification of p116<sup>RIP3</sup> interaction with Rac1 and RhoA. B, Co-immunoprecipitation of endogenous p116<sup>RIP3</sup> with the indicated Rac1 mutants transfected in vSMC (n=4). C, Co-immunoprecipitation of endogenous p116<sup>RIP3</sup> with PKG in murine aortas stimulated with SNP. D, Time-course of SNP-induced RhoA phosphorylation on Ser188 and p116<sup>RIP3</sup>-RhoA complex formation assessed in immunoprecipitated RhoA from vSMC. E, Co-immunoprecipitation of endogenous p116<sup>RIP3</sup> with the phosphomimetic (GFP-RhoA<sup>S188E</sup>), phosphoresistant (GFP-RhoA<sup>S188A</sup>) or wild type (GFP-RhoA<sup>WT</sup>) RhoA in transfected vSMC in the absence or presence of SNP (n=5). \*P<0.05. GFP indicates Green Fluorescent Protein; Ig, Immunoglobulin; IP, immunoprecipitation; PKG, protein kinase G; Rho, Ras homologous; TCL, total cell lysate; vSMC, vascular smooth muscle cells; WT, wild type.

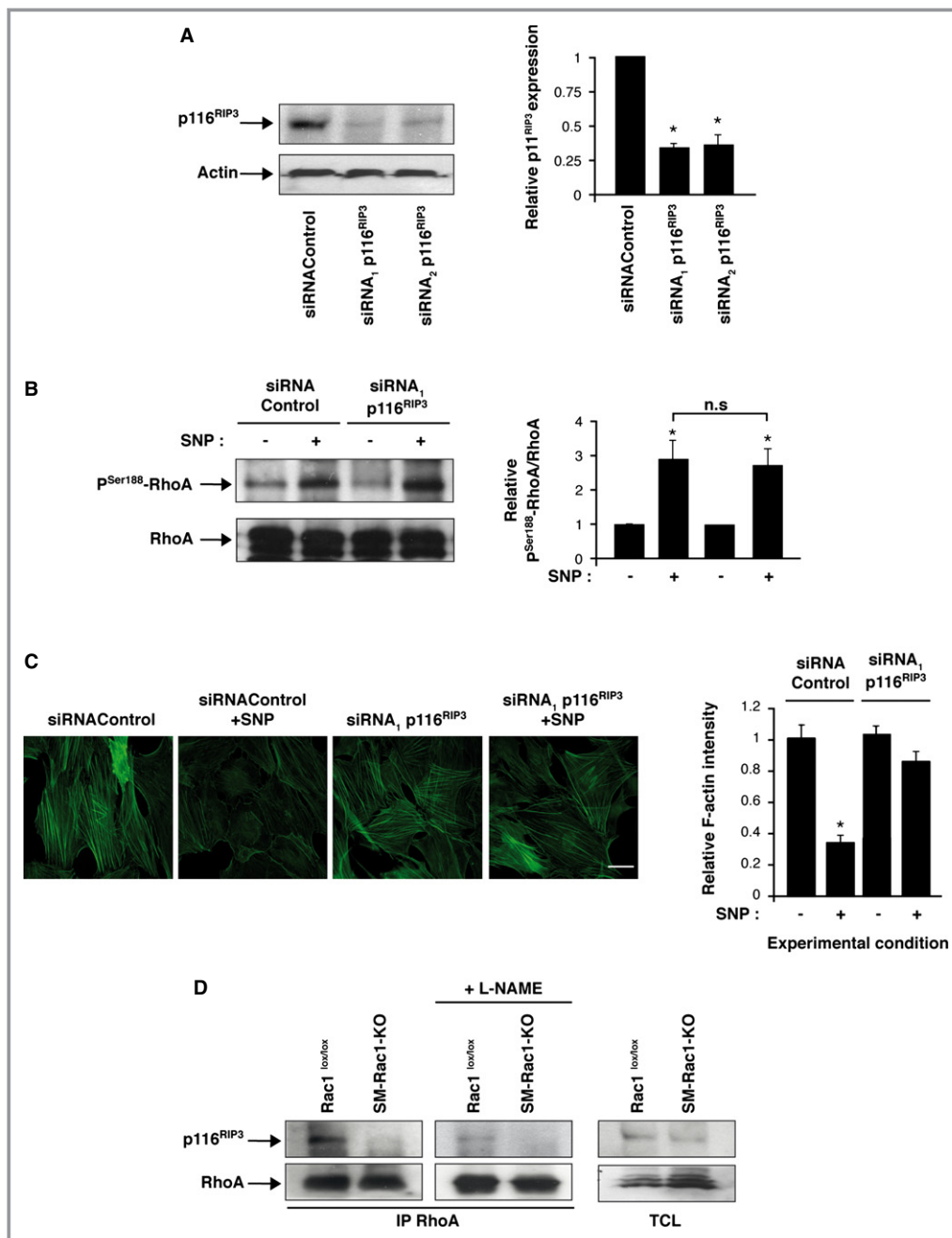


**Figure 6.** Down-regulation of p116<sup>RIP3</sup> expression in vSMC prevents NO-dependent RhoA inactivation. A, Inhibition of p116<sup>RIP3</sup> protein expression by RNA interference (siRNA) assessed by immunoblot in vSMC (n=3). B, Immunoblot analysis of NO-dependent RhoA phosphorylation (P<sup>Ser188</sup>) in p116<sup>RIP3</sup> siRNA transfected vSMC (n=3). C, Effect of p116<sup>RIP3</sup> siRNA on F-actin cytoskeleton organization with or without SNP treatment in vSMC (n=4). D, Endogenous p116<sup>RIP3</sup> in RhoA immunoprecipitates obtained from aortas of Rac1<sup>lox/lox</sup> and SM-Rac1-KO mice treated or not with L-NAME (3 g/L in drinking water) (n=8). \*P<0.05. IP indicates immunoprecipitation; NO, nitric oxide; Rho, Ras homologous; SM-Rac1, smooth muscle Rac1 knockout; TCL, total cell lysate; vSMC, vascular smooth muscle cells.

## Discussion

Our study identifies a new role of Rac1 as a regulator of blood pressure and a key component of the signaling pathway that mediates the blood pressure-lowering effect of NO in vSMC.

We demonstrate that ablation of the *Rac1* gene in vSMC is sufficient to induce high blood pressure in mice, supporting a physiological role of vSMC Rac1 in blood pressure homeostasis. Moreover, we found that Rac1 is a molecular link connecting NO to cGMP and RhoA signaling inhibition, and

discovered the key role of p116<sup>RIP3</sup> in this pathway essential for NO-mediated vasodilation (Figure 7).

SM-Rac1-KO mice display a ≈15 mm Hg increase in blood pressure associated with a specific loss of NO-mediated increase in cGMP and vasodilation. Moreover, mutant mice are resistant to L-NAME-induced rise in blood pressure. The role of Rac1 in the regulation of NO/cGMP signaling and the causative effect of Rac1 deletion-induced defective NO signaling in the pathogenesis of hypertension in SM-Rac1-KO mice are supported by previous studies showing that *eNOS* or *PKG* gene disruption in mice similarly led to the abrogation of

NO/cGMP-dependent arterial relaxation and an increase in arterial pressure of about 10 to 15 mm Hg.<sup>36–39</sup> In addition to an increase in arterial pressure, this alteration of NO signaling could also account for the rise of arterial stiffness observed in SM-Rac1-KO mice as a chronic reduction of NO production induced vascular stiffening.<sup>40,41</sup> This close relationship between high systolic blood pressure, endothelial dysfunction, and vascular elastance was also found in hypertensive patients<sup>42</sup> and aging population.<sup>43–45</sup> All these data are thus consistent with an essential role of Rac1 to mediate NO effect in vSMC and consequently, NO-dependent regulation of

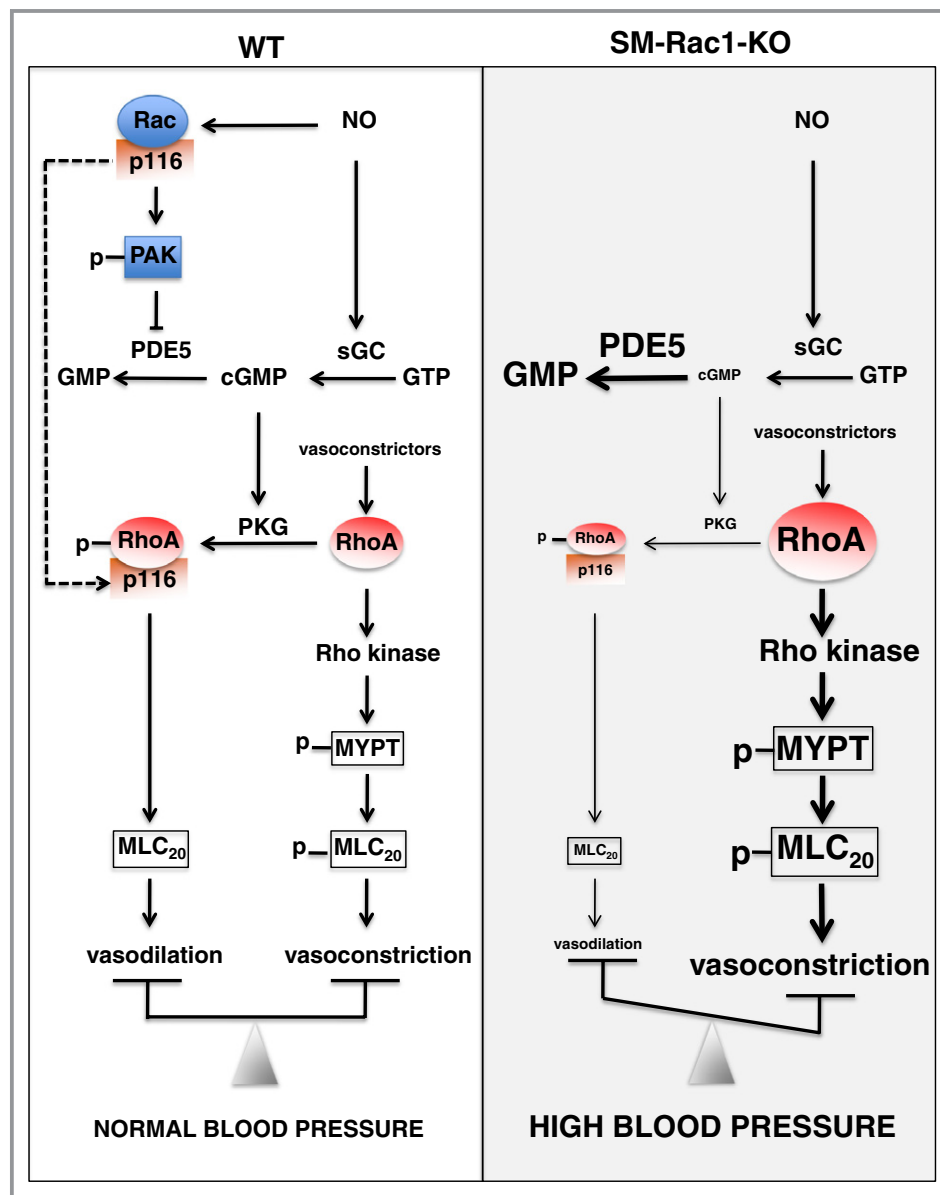


**Figure 7.** Schematics representations of the new regulatory mechanism reported in this work. MLC indicates myosin light chain; PAK1, p21-activated kinase 1; PDE5, type 5 phosphodiesterase; Rho, Ras homologous; sGC, soluble guanylyl cyclases; SM-Rac1, smooth muscle Rac1 knockout; WT, wild type.

vascular tone and blood pressure. In agreement with our finding, it was recently found that the Ala370Ser polymorphism in the *ARHGAP9* gene coding for a RacGAP inactivating Rac1, is associated with coronary artery spasm in human ascribed to a decreased GAP activity towards Rac1.<sup>46</sup>

In mice, overexpression of a dominant-negative or a constitutively active mutant of Rac1 gene in SMC has shown that Rac1 is an essential regulator of NADPH oxidase/ROS pathway in blood vessels.<sup>47,48</sup> While blood pressure has not been measured in transgenic mice overexpressing the dominant-negative form of Rac1, animals that overexpressed the active Rac1 mutant in vSMC developed moderate hypertension due to an excessive amounts of  $O_2^{\bullet-}$ ,<sup>48</sup> Therefore, it is surprising that overexpression of active Rac1 mutant and deletion of endogenous Rac1 in SMC lead to the same blood pressure phenotype. A possible explanation is that the massive artificial ROS production due to Rac1 overexpression completely masks the physiological role of endogenous Rac1 as a component of the NO/cGMP signaling in vSMC.

In SM-Rac1-KO mice, the inability of vSMC to normally respond to NO resulted from a defective production of cGMP.<sup>34,49,50</sup> Although Rac1 has been shown to positively control sGC expression in adipocytes,<sup>50</sup> we did not observe any modification of sGC $\alpha$ 1 and sGC $\beta$ 1 expression in SM-Rac1-KO aorta suggesting that the low level of cGMP in SM-Rac1-KO mice arteries was not due to a defect in cGMP generation. However, we show that NO induces activation of Rac1 and formation of Pak1/PDE5 complex in vSMC. The loss of Pak1/PDE5 interaction in response to NO donor observed in SM-Rac1-KO mice arteries is likely responsible for the decrease in cGMP level by preventing NO-induced inhibition of cGMP hydrolysis.

Arterial blood pressure depends in part on the regulation of blood vessel lumen diameter, determined by the contractile activity of vSMC. The RhoA/Rho kinase signaling pathway plays a major role in the  $Ca^{2+}$ -independent contraction of vSMC and the regulation of vascular tone and blood pressure by vasoconstrictors.<sup>18,51–53</sup> Conversely, inhibition of RhoA/Rho kinase signaling by NO, through PKG-mediated phosphorylation of RhoA on Ser188, plays a major role in the relaxing effect of NO in vSMC.<sup>54–56</sup> In agreement with the involvement of this pathway in vivo, the depression of NO signaling in SM-Rac1-KO mice arteries is associated with an increase in RhoA/Rho kinase activity attested by a rise of MYPT phosphorylation and a decreased phosphorylation of RhoA on Ser188. Deletion of Rac1 in SMC thus mimics the activation of RhoA/Rho kinase signaling observed in hypertensive *eNOS*-deficient mice.<sup>57,58</sup> This higher activity of RhoA/Rho kinase in SM-Rac1-KO mice arteries is consistent with the potentiation of contractile responses of resistance arteries to the thromboxane A2 analog U47619 and Phe, whereas  $Ca^{2+}$ -dependent  $K^+$ -contractions are unchanged.

In an attempt to decipher the molecular pathway linking Rac1 to RhoA regulation, we identified the protein p116<sup>RIP3</sup>. p116<sup>RIP3</sup> was initially described as a component of MLCP complex that directly binds RhoA.<sup>35</sup> Overexpression of p116<sup>RIP3</sup> disrupts the actin cytoskeleton and inhibits contractility by activating MLCP and inactivating RhoA.<sup>59–63</sup> The interaction between RhoA and p116<sup>RIP3</sup> occurs independently of the nucleotide binding state of RhoA and the regulation of this complex formation as well as its physiological role are totally unknown.<sup>35</sup> Here we demonstrate that stimulation of NO pathway promotes Rac1-p116<sup>RIP3</sup> dissociation and RhoA-p116<sup>RIP3</sup> complex formation that is favored by RhoA phosphorylation. In addition, we demonstrated that despite its association to PKG, p116<sup>RIP3</sup> is not involved in NO-induced RhoA phosphorylation but is essential to mediate the inhibitory action of NO on RhoA/Rho kinase activity. These data thus identified p116<sup>RIP3</sup> as a new and essential intermediate in the signaling pathway responsible for cGMP/PKG-mediated inhibition of RhoA cellular functions. By preventing NO-induced p116<sup>RIP3</sup>-RhoA interaction, Rac1 deletion disrupts NO-mediated inhibition of RhoA/Rho kinase effects in vSMC, leading to RhoA/Rho kinase-dependent increase in arterial tone and blood pressure. Vascular SMC Rac1 thus constitutively acts as a brake that limits RhoA/Rho kinase activity in response to NO.

Finally, our present data highlight a functional significance of the reciprocal antagonistic relationship between Rac1 and RhoA at a physiological level, ie, blood pressure regulation. The blood pressure-lowering effect of vSMC Rac1 opposes the hypertensive effect of vSMC RhoA. Rac1 is required for NO/cGMP/PKG/p116<sup>RIP3</sup>-mediated inactivation of RhoA that in turn activates Rac1.<sup>9</sup> This positive feedback creates a virtuous circle that contributes to the balance between vasodilation and vasoconstriction and efficiently regulates blood pressure.

## Acknowledgments

We thank N. Vaillant, V. Aillerie, M. Rio, and S. Heurtebise-Chretien for excellent technical assistance. We also value the support provided by the animal facility units of the University of Nantes. We thank Cardiex platform for the cardiovascular expertise and the INRA Research Unit 1268 for the mass spectrometry analyses.

## Sources of Funding

This work was supported by grants from the Agence National de la Recherche (project number ANR-09-JCJC-0115-01) and from the Institut National de la Santé et de la Recherche Médicale (INSERM). André was supported by a grant from MRES. The authors of the manuscript do not have any competing financial interests in any of the data reported.

## Disclosures

None.

## References

- Bustelo XR, Ojeda V, Barreira M, Sauzeau V, Castro-Castro A. Rac-ing to the plasma membrane: the long and complex work commute of rac1 during cell signaling. *Small GTPases*. 2012;3:60–66.
- Bustelo XR, Sauzeau V, Berenjano IM. Gtp-binding proteins of the rho/rac family: regulation, effectors and functions in vivo. *BioEssays*. 2007;29:356–370.
- Heasman SJ, Ridley AJ. Mammalian rho gtpases: new insights into their functions from in vivo studies. *Nat Rev Mol Cell Biol*. 2008;9:690–701.
- Ridley AJ, Hall A. The small gtp-binding protein rho regulates the assembly of focal adhesions and actin stress fibers in response to growth factors. *Cell*. 1992;70:389–399.
- Guo F, Debidda M, Yang L, Williams DA, Zheng Y. Genetic deletion of rac1 gtpase reveals its critical role in actin stress fiber formation and focal adhesion complex assembly. *J Biol Chem*. 2006;281:18652–18659.
- Ohta Y, Hartwig JH, Stossel TP. Filgap, a rho- and rock-regulated gap for rac binds filamin a to control actin remodelling. *Nat Cell Biol*. 2006;8:803–814.
- Guilluy C, Garcia-Mata R, Burrige K. Rho protein crosstalk: another social network? *Trends Cell Biol*. 2011;21:718–726.
- Machacek M, Hodgson L, Welch C, Elliott H, Pertz O, Nalbant P, Abell A, Johnson GL, Hahn KM, Danuser G. Coordination of rho gtpase activities during cell protrusion. *Nature*. 2009;461:99–103.
- Rolli-Derkinderen M, Toumaniantz G, Pacaud P, Loirand G. Rho phosphorylation induces rac1 release from guanine dissociation inhibitor alpha and stimulation of vascular smooth muscle cell migration. *Mol Cell Biol*. 2010;30:4786–4796.
- Laufs U, Liao JK. Post-transcriptional regulation of endothelial nitric oxide synthase mrna stability by rho gtpase. *J Biol Chem*. 1998;273:24266–24271.
- Wolfrum S, Dendorfer A, Rikitake Y, Stalker TJ, Gong Y, Scalia R, Dominiak P, Liao JK. Inhibition of rho-kinase leads to rapid activation of phosphatidylinositol 3-kinase/protein kinase akt and cardiovascular protection. *Arterioscler Thromb Vasc Biol*. 2004;24:1842–1847.
- Sawada N, Salomone S, Kim HH, Kwiatkowski DJ, Liao JK. Regulation of endothelial nitric oxide synthase and postnatal angiogenesis by rac1. *Circ Res*. 2008;103:360–368.
- Selvakumar B, Hess DT, Goldschmidt-Clermont PJ, Stamler JS. Co-regulation of constitutive nitric oxide synthases and nadph oxidase by the small gtpase rac. *FEBS Lett*. 2008;582:2195–2202.
- Adamson RH, Sarai RK, Clark JF, Altangerel A, Thirkill TL, Curry FE. Attenuation by sphingosine-1-phosphate of rat microvessel acute permeability response to bradykinin is rapidly reversible. *Am J Physiol Heart Circ Physiol*. 2012;302:H1929–H1935.
- Monaghan-Benson E, Burrige K. The regulation of vascular endothelial growth factor-induced microvascular permeability requires rac and reactive oxygen species. *J Biol Chem*. 2009;284:25602–25611.
- Gavard J, Gutkind JS. Vegf controls endothelial-cell permeability by promoting the beta-arrestin-dependent endocytosis of ve-cadherin. *Nat Cell Biol*. 2006;8:1223–1234.
- Loirand G, Guerin P, Pacaud P. Rho kinases in cardiovascular physiology and pathophysiology. *Circ Res*. 2006;98:322–334.
- Loirand G, Pacaud P. The role of rho protein signaling in hypertension. *Nat Rev Cardiol*. 2010;7:637–647.
- Shirai HAM, Eguchi S. Small gtp-binding proteins and mitogen-activated protein kinases as promising therapeutic targets of vascular remodeling. *Curr Opin Nephrol Hypertens*. 2007;16:111–115.
- Sanders LC, Matsumura F, Bokoch GM, de Lanerolle P. Inhibition of myosin light chain kinase by p21-activated kinase. *Science*. 1999;283:2083–2085.
- Wirth A, Schroeter M, Kock-Hauser C, Manser E, Chalovich JM, De Lanerolle P, Pfizter G. Inhibition of contraction and myosin light chain phosphorylation in guinea-pig smooth muscle by p21-activated kinase 1. *J Physiol*. 2003;549:489–500.
- Foster DB, Shen LH, Kelly J, Thibault P, Van Eyk JE, Mak AS. Phosphorylation of caldesmon by p21-activated kinase. Implications for the ca(2+) sensitivity of smooth muscle contraction. *J Biol Chem*. 2000;275:1959–1965.
- Rahman A, Davis B, Lovdahl C, Hanumaiah VT, Feil R, Brakebusch C, Amer A. The small gtpase rac1 is required for smooth muscle contraction. *J Physiol*. 2014;592:(Pt 5)915–926.
- Sauzeau V, Sevilla MA, Rivas-Elena JV, de Alava E, Montero MJ, Lopez-Novoa JM, Bustelo XR. Vav3 proto-oncogene deficiency leads to sympathetic hyperactivity and cardiovascular dysfunction. *Nat Med*. 2006;12:841–845.
- Sauzeau V, Jerkic M, Lopez-Novoa JM, Bustelo XR. Loss of vav2 proto-oncogene causes tachycardia and cardiovascular disease in mice. *Mol Biol Cell*. 2007;18:943–952.
- Wirth A, Benyo Z, Lukasova M, Leutgeb B, Wettshureck N, Gorbey S, Orsy P, Horvath B, Maser-Gluth C, Greiner E, Lemmer B, Schutz G, Gutkind JS, Offermanns S. G12-G13-larg-mediated signaling in vascular smooth muscle is required for salt-induced hypertension. *Nat Med*. 2008;14:64–68.
- Guilluy C, Bregeon J, Toumaniantz G, Rolli-Derkinderen M, Retailleau K, Loufrani L, Henrion D, Scalbert E, Brill A, Torres RM, Offermanns S, Pacaud P, Loirand G. The rho exchange factor arhgef1 mediates the effects of angiotensin ii on vascular tone and blood pressure. *Nat Med*. 2010;16:183–190.
- Mills PA, Huetteman DA, Brockway BP, Zwiers LM, Gelsema AJ, Schwartz RS, Kramer K. A new method for measurement of blood pressure, heart rate, and activity in the mouse by radiotelemetry. *J Appl Physiol*. 2000;88:1537–1544.
- Loufrani L, Levy BI, Henrion D. Defect in microvascular adaptation to chronic changes in blood flow in mice lacking the gene encoding for dystrophin. *Circ Res*. 2002;91:1183–1189.
- Guilluy C, Dubash AD, Garcia-Mata R. Analysis of rhoa and rho gef activity in whole cells and the cell nucleus. *Nat Protoc*. 2011;6:2050–2060.
- Gayard M, Guilluy C, Rousselle A, Viollet B, Henrion D, Pacaud P, Loirand G, Rolli-Derkinderen M. Ampk alpha 1-induced rhoa phosphorylation mediates vasoprotective effect of estradiol. *Arterioscler Thromb Vasc Biol*. 2011;31:2634–2642.
- Lifton RP, Gharavi AG, Geller DS. Molecular mechanisms of human hypertension. *Cell*. 2001;104:545–556.
- Sauzeau V, Le Jeune H, Cario-Toumaniantz C, Smolenski A, Lohmann SM, Bertoglio J, Chardin P, Pacaud P, Loirand G. Cyclic gmp-dependent protein kinase signaling pathway inhibits rhoa-induced ca2+ sensitization of contraction in vascular smooth muscle. *J Biol Chem*. 2000;275:21722–21729.
- Sauzeau V, Sevilla MA, Montero MJ, Bustelo XR. The rho/rac exchange factor vav2 controls nitric oxide-dependent responses in mouse vascular smooth muscle cells. *J Clin Invest*. 2010;120:315–330.
- Surks HK, Richards CT, Mendelsohn ME. Myosin phosphatase-rho interacting protein. A new member of the myosin phosphatase complex that directly binds rhoa. *J Biol Chem*. 2003;278:51484–51493.
- Shesely EG, Maeda N, Kim HS, Desai KM, Kregge JH, Laubach VE, Sherman PA, Sessa WC, Smithies O. Elevated blood pressures in mice lacking endothelial nitric oxide synthase. *Proc Natl Acad Sci USA*. 1996;93:13176–13181.
- Stauss HM, Godecke A, Mrowka R, Schrader J, Persson PB. Enhanced blood pressure variability in enos knockout mice. *Hypertension*. 1999;33:1359–1363.
- Van Vliet BN, Chafe LL, Montani JP. Characteristics of 24 h telemetered blood pressure in enos-knockout and c57bl/6j control mice. *J Physiol*. 2003;549:313–325.
- Pfeifer A, Klatt P, Massberg S, Ny L, Sausbier M, Hirneiss C, Wang GX, Korh M, Aszodi A, Andersson KE, Krombach F, Mayerhofer A, Ruth P, Fassler R, Hofmann F. Defective smooth muscle regulation in cgmp kinase i-deficient mice. *EMBO J*. 1998;17:3045–3051.
- Isabelle M, Simonet S, Ragonnet C, Sansilvestri-Morel P, Clavreul N, Vayssettes-Courchay C, Verbeuren TJ. Chronic reduction of nitric oxide level in adult spontaneously hypertensive rats induces aortic stiffness similar to old spontaneously hypertensive rats. *J Vasc Res*. 2012;49:309–318.
- Nakmareong S, Kukongviriyapan U, Pakdeechote P, Kukongviriyapan V, Kongyingyoes B, Donpunha W, Prachaney P, Phisalaphong C. Tetrahydrocurcumin alleviates hypertension, aortic stiffening and oxidative stress in rats with nitric oxide deficiency. *Hypertens Res*. 2012;35:418–425.
- Figueiredo VN, Yugar-Toledo JC, Martins LC, Martins LB, de Faria AP, de Haro Moraes C, Sierra C, Coca A, Moreno H. Vascular stiffness and endothelial dysfunction: correlations at different levels of blood pressure. *Blood Press*. 2012;21:31–38.
- Sindler AL, Fleenor BS, Calvert JW, Marshall KD, Zigler ML, Lefer DJ, Seals DR. Nitrite supplementation reverses vascular endothelial dysfunction and large elastic artery stiffness with aging. *Aging Cell*. 2011;10:429–437.
- Wilkinson IB, Franklin SS, Cockcroft JR. Nitric oxide and the regulation of large artery stiffness: from physiology to pharmacology. *Hypertension*. 2004;44:112–116.
- Brandes RP, Fleming I, Busse R. Endothelial aging. *Cardiovasc Res*. 2005;66:286–294.
- Takefuji M, Asano H, Mori K, Amano M, Kato K, Watanabe T, Morita Y, Katsumi A, Itoh T, Takenawa T, Hirashiki A, Izawa H, Nagata K, Hirayama H, Takatsu F, Naoe T, Yokota M, Kaibuchi K. Mutation of arhgap9 in patients with coronary spastic angina. *J Hum Genet*. 2010;55:42–49.

47. Nowicki PT, Flavahan S, Hassanain H, Mitra S, Holland S, Goldschmidt-Clermont PJ, Flavahan NA. Redox signaling of the arteriolar myogenic response. *Circ Res*. 2001;89:114–116.
48. Hassanain HH, Gregg D, Marcelo ML, Zweier JL, Souza HP, Selvakumar B, Ma Q, Moustafa-Bayoumi M, Binkley PF, Flavahan NA, Morris M, Dong C, Goldschmidt-Clermont PJ. Hypertension caused by transgenic overexpression of rac1. *Antioxid Redox Signal*. 2007;9:91–100.
49. Guo D, Zhang JJ, Huang XY. A new rac/pak/gc/cgmp signaling pathway. *Mol Cell Biochem*. 2010;334:99–103.
50. Jennissen K, Siegel F, Liebig-Gonglach M, Hermann MR, Kipschull S, van Dooren S, Kunz WS, Fassler R, Pfeifer A. A vasp-rac-soluble guanylyl cyclase pathway controls cgmp production in adipocytes. *Sci Signal*. 2012;5:ra62.
51. Baek EB, Kim SJ. Mechanisms of myogenic response: Ca(2+)-dependent and -independent signaling. *J Smooth Muscle Res*. 2011;47:55–65.
52. Hilgers RH, Webb RC. Molecular aspects of arterial smooth muscle contraction: focus on rho. *Exp Biol Med (Maywood)*. 2005;230:829–835.
53. Wang Y, Zheng XR, Riddick N, Bryden M, Baur W, Zhang X, Surks HK. Rock isoform regulation of myosin phosphatase and contractility in vascular smooth muscle cells. *Circ Res*. 2009;104:531–540.
54. Somlyo AP, Somlyo AV. Ca<sup>2+</sup> sensitivity of smooth muscle and nonmuscle myosin ii: modulated by g proteins, kinases, and myosin phosphatase. *Physiol Rev*. 2003;83:1325–1358.
55. Bolz SS, Vogel L, Sollinger D, Derwand R, de Wit C, Loirand G, Pohl U. Nitric oxide-induced decrease in calcium sensitivity of resistance arteries is attributable to activation of the myosin light chain phosphatase and antagonized by the rhoa/rho kinase pathway. *Circulation*. 2003;107:3081–3087.
56. Sauzeau V, Le Jeune H, Cario-Toumaniantz C, Vaillant N, Gadeau AP, Desgranges C, Scalbert E, Chardin P, Pacaud P, Loirand G. P2y(1), p2y(2), p2y(4), and p2y(6) receptors are coupled to rho and rho kinase activation in vascular myocytes. *Am J Physiol Heart Circ Physiol*. 2000;278:H175–H1761.
57. Priviero FB, Jin LM, Ying Z, Teixeira CE, Webb RC. Up-regulation of the rhoa/rho-kinase signaling pathway in corpus cavernosum from endothelial nitric-oxide synthase (nos), but not neuronal nos, null mice. *J Pharmacol Exp Ther*. 2010;333:184–192.
58. Williams J, Bogwu J, Oyekan A. The role of the rhoa/rho-kinase signaling pathway in renal vascular reactivity in endothelial nitric oxide synthase null mice. *J Hypertens*. 2006;24:1429–1436.
59. Gebbink MF, Kranenburg O, Poland M, van Horck FP, Houssa B, Moolenaar WH. Identification of a novel, putative rho-specific gdp/gtp exchange factor and a rhoa-binding protein: control of neuronal morphology. *J Cell Biol*. 1997;137:1603–1613.
60. Mulder J, Poland M, Gebbink MF, Calafat J, Moolenaar WH, Kranenburg O. P116rip is a novel filamentous actin-binding protein. *J Biol Chem*. 2003;278:27216–27223.
61. Koga Y, Ikebe M. P116rip decreases myosin ii phosphorylation by activating myosin light chain phosphatase and by inactivating rhoa. *J Biol Chem*. 2005;280:4983–4991.
62. Mulder J, Ariaens A, van Horck FP, Moolenaar WH. Inhibition of rhoa-mediated srf activation by p116rip. *FEBS Lett*. 2005;579:6121–6127.
63. Vallenius T, Vaahtomeri K, Kovac B, Osiceanu AM, Viljanen M, Makela TP. An association between nuak2 and mrip reveals a novel mechanism for regulation of actin stress fibers. *J Cell Sci*. 2011;124:384–393.